Appendix A.29:

Barrington Park – VsVp 38172

Table 1: Site Description for Barrington Park (VsVp 38172).

Attribute	Yes/No			Description/Date	Symbol in Figure 1
	10-m Buffer	20-m Buffer	50-m Buffer		
Near a body of surface water or other free face features?	No	No	No	The center of the site is 950 meters away from the Heathcote River. The direction of the free face is roughly NW-SE, while its height is ~2.5 m.	NA
Lateral spreading observed during the CES?	No	No	No	No lateral spreading was observed by the mapping team.[1]	NA
Nearby buildings or structures?	No	No	Yes	Buildings occupy ~10% of the E portion of the 50-m buffer.	White Fill + Brown Outline
Sloping land?	No	No	No	Flat land, open + residential area	NA
Step changes in the ground surface?	No	No	No	NA	NA
Retaining walls?	No	No	No	NA	NA
Vegetation?	Yes	Yes	Yes	Trees and bushes cover 12, 28, and 18% of the 10-, 20-, and 50-m buffers, respectively. They are in all quadrants of the 20- and 50-m buffers and the NW and SE quadrants of the 10-m buffer.	White Fill + Green Outline
Anthropogenic changes to the site between the LiDAR surveys?	No	Yes	Yes	Building addition in the SE quadrant of the 50-m buffer between Jan 2005 and Jan 2006. Tree removal in the SE quadrant of the 50-m buffer between Mar 2009 and Oct 2009. Earthwork in the S portion of the 20- and 50-m buffers between 28 Mar 2011 and Aug 2011. Vegetation removal in the E portion of the 50-m buffer between Mar 2013 and Aug 2013.	Building Addition: Orange Crossline; Vegetation Removal: Green Crossline
Other important factors?	No	Yes	Yes	The S portion of the 20- and 50-m buffers is part of the rugby field that is a subject to grass replacement.	NA

Note: Buffer is the area within a circle of a specified radius with CPT investigations done at its center (172.617541°, -43.554035°).

[1] Canterbury Geotechnical Database. (2012). "Observed Ground Crack Locations", Map Layer CGD0400 - 23 July 2012, retrieved July 09, 2018 from https://canterburygeotechnicaldatabase.projectorbit.com/

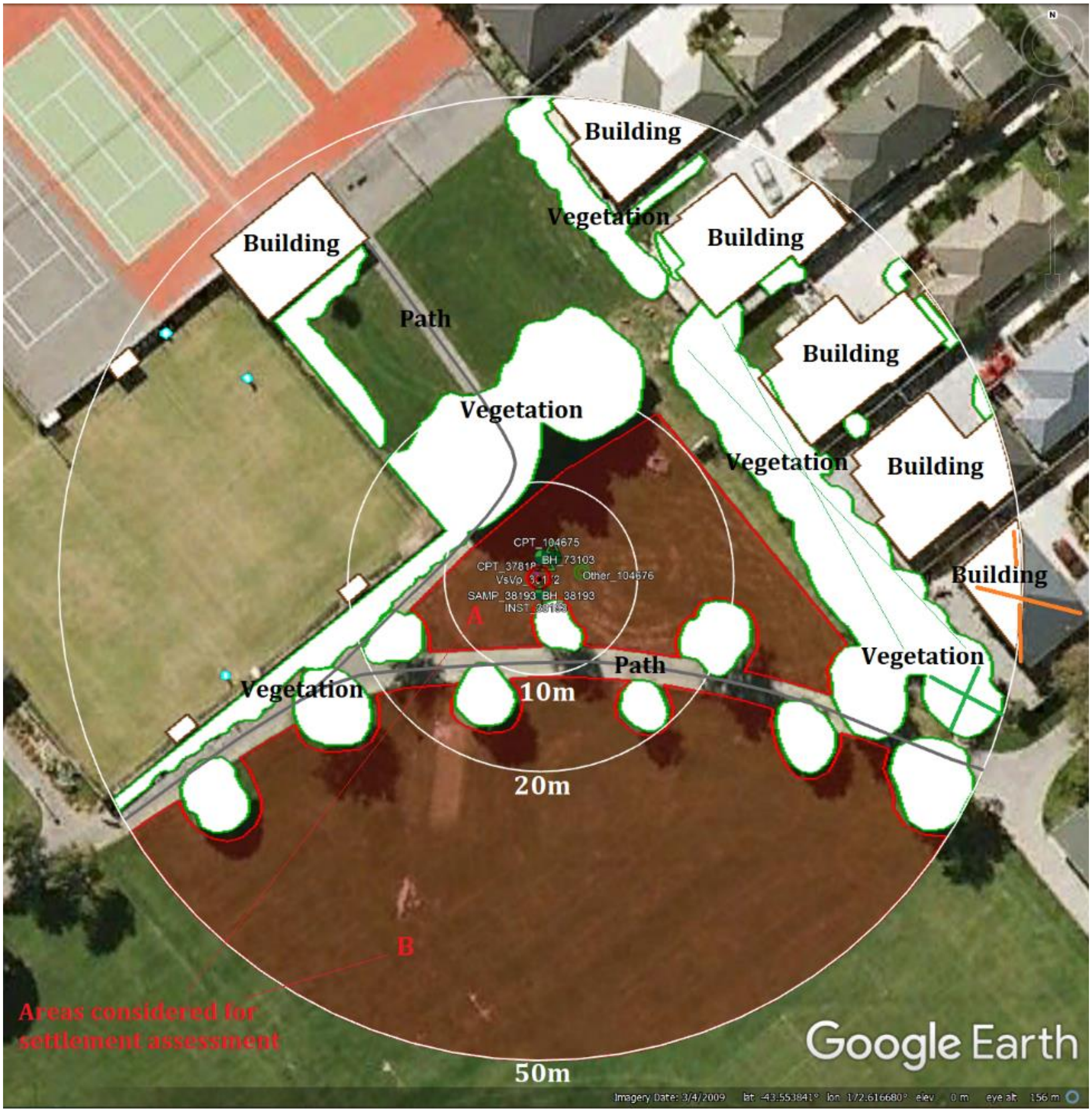

Figure 1: Site plan with areas where ejecta-induced settlement is considered.

Note 1: Two patches (outlined in red) in free field were selected for settlement assessment as areas free of vegetation and structures. Other factors considered in the selection process were the proximity of a patch to a CPT, a property subjected to addition and/or demolition of a structure, front yard/backyard alterations (e.g., ploughing, rubble, scrap), and aerial distribution of sediment ejecta. Due to the evident absence of ejecta from Patches A and B for the Sep-10, Jun-11, and Dec-11 EQs and the unavailability of the LiDAR surveys for the Feb-11 EQ, the LiDAR-based settlement analyses were not conducted.

Table 2: LiDAR flight error adjustments, global adjustments for the difference between average LiDAR point elevations and benchmark survey elevations, and vertical tectonic movement adjustments.

	Adjustments (mm)		
Earthquake Event(s)	LiDAR Flight Error	Global Offset[2]	Tectonic Vertical Movement
Sep-10	NA	-3	0
Feb-11	NA	16	-80
Jun-11	0	38	-25
Dec-11	NA	-65	+10
CES	NA	-14	-95
Any LiDAR survey affected by ejecta?			No

Note: The negative sign indicates the subtraction from the ground surface subsidence, while the positive sign indicates the addition to the ground surface subsidence.

Table 3: LiDAR Measurement Error for Patches A and B.

Surveys	Buffer	Area Averaged Difference Indicating Repeat Measurement Error (mm)	ϭ*$_{individual}$ LiDAR points (mm)	%Reduction in ϭ due to Area Averaging of LiDAR Points
Post Feb 2011: Mar 2011 and May 2011	10-m	ND/NA	59	[ND,ND]
	20-m	ND		
	50-m	ND		
Post Dec 2011: Feb 2012 and Oct 2015	10-m	NA	70	[NA,NA]
	20-m	NA		
	50-m	NA		

*Standard deviation; ND = Not determined; NA = Not available.

[2] Russell, J., & van Ballegooy, S. (2015). *Canterbury Earthquake Sequence: Increased liquefaction vulnerability assessment methodology*. New Zealand: Tonkin & Taylor Ltd.

Table 4: Ground surface subsidence adjustments due to LiDAR measurement error for Patches A and B.

Earthquake Event(s)	$\sigma_{\text{pre-EQ LiDAR survey}}$ (mm)	$\sigma_{\text{post-EQ LiDAR survey}}$ (mm)	σ_{total} (mm)	Area Average Adjusted σ (mm) **
Sep-10	158	56	134	ND
Feb-11	56	59	59	ND
Jun-11	59	61	62	ND
Dec-11	61	70	87	ND
CES	158	70	124	ND

**Based on the highest %Reduction in Table 3.

Table 5: Raw liquefaction-related ground surface subsidence using original LiDAR points for Patches A and B.

	Average Ground Surface Subsidence (mm)		
Earthquake Event(s)	10-m Buffer	20-m Buffer	50-m Buffer
Sep-10	NA	NA	NA
Feb-11	NA	NA	NA
Jun-11	ND/NA	ND	ND
Dec-11	ND/NA	ND	ND
CES	ND/NA	ND	ND

Table 6: Corrected liquefaction-related ground surface subsidence using original LiDAR points for Patches A and B with the calculated adjustments in Table 2.

	Average Calculated Ground Surface Subsidence (mm)		
Earthquake Event(s)	10-m Buffer	20-m Buffer	50-m Buffer
Sep-10	NA	NA	NA
Feb-11	NA	NA	NA
Jun-11	ND/NA	ND	ND
Dec-11	ND/NA	ND	ND
CES	ND/NA	ND	ND

Notes: Plus/minus values are same as those in Table 4, but rounded to the nearest 25; Positive overall values indicate ground surface subsidence, while negative overall values indicate ground surface uplift.

Table 7a: Corrected liquefaction-related ground surface subsidence for Patch A using LiDAR DEMs.

	Estimated Ground Surface Subsidence (mm)								
	10-m Buffer			20-m Buffer			50-m Buffer		
Earthquake Event(s)	16^{th} %ile	50^{th} %ile	84^{th} %ile	16^{th} %ile	50^{th} %ile	84^{th} %ile	16^{th} %ile	50^{th} %ile	84^{th} %ile
Sep-10	NA	NA	NA	NA	NA	NA	NA	NA	NA
Feb-11	NA	NA	NA	NA	NA	NA	NA	NA	NA
Jun-11	<50	<50	<50	<50	<50	<50	<50	<50	<50
Dec-11	NA	NA	NA	NA	NA	NA	NA	NA	NA
CES	NA	NA	NA	NA	NA	NA	NA	NA	NA

Note: These percentiles are not the exact statistical measures; they indicate the spatial variability of ground surface subsidence.

Table 7b: Corrected liquefaction-related ground surface subsidence for Patch B using LiDAR DEMs.

	Estimated Ground Surface Subsidence (mm)								
	10-m Buffer			20-m Buffer			50-m Buffer		
Earthquake Event(s)	16^{th} %ile	50^{th} %ile	84^{th} %ile	16^{th} %ile	50^{th} %ile	84^{th} %ile	16^{th} %ile	50^{th} %ile	84^{th} %ile
Sep-10	NA	NA	NA	NA	NA	NA	NA	NA	NA
Feb-11	NA	NA	NA	NA	NA	NA	NA	NA	NA
Jun-11	NA	NA	NA	<50	<50	<50	<50	<50	<50
Dec-11	NA	NA	NA	NA	NA	NA	NA	NA	NA
CES	NA	NA	NA	NA	NA	NA	NA	NA	NA

Note: These percentiles are not the exact statistical measures; they indicate the spatial variability of ground surface subsidence.

Table 8: Ejecta-Induced settlement for the top 20 m of the soil profile for Patches A and B for the 50th %ile PGA, P_L=50%, and C_{FC}=0.13 using BI-2014, ZRB-2002, and I_C cutoff of 2.6.

Earthquake Event(s)	M_W	PGA (g)	Depth to Groundwater (m)	S_T (mm)	S_{V1D} (mm)	$S_{E,L}$ (mm)
Sep-10	7.1	0.23	0.5	NA	94±20	NA
Feb-11	6.2	0.42	0.5	NA	119±50	NA
Jun-11	6.2	0.20	0.5	ND	54±25	ND
Dec-11	6.1	0.16	0.5	ND	21±50	ND

Notes: S_T = Total settlement (Table 6); S_{V1D} = Average vertical settlement due to volumetric compression using Boulanger and Idriss (2014) (BI-2014), Zhang et al. (2002) (ZRB-2002) procedures and de Greef and Lengkeek (2018) thin-layer correction; $S_{E,L}$ = Ejecta-induced settlement as the difference between the LiDAR-based S_T and S_{V1D}.

Note 2: The uncertainty for volumetric settlement was derived based on the sensitivity of volumetric settlement to PGA, C_{FC}, and P_L for each earthquake event for VsVp 57203 *Shirley Intermediate School* and CC LIQ 1 – CPT 5586 – *Vivian St* sites. Taking the 50th percentile as the baseline case, the minimum and maximum values corresponding to the difference between the 25th percentile and the 50th percentile and the 75th percentile and the 50th percentile were determined. The arithmetic mean of the range of the minimum and maximum difference was evaluated for each patch at the two sites. The maximum arithmetic mean for each earthquake event was rounded to the nearest five and used as the uncertainty value. Accordingly, the 1-D volumetric settlement uncertainties of ±20, ±50, ±25, and ±50 mm for the Sep-10, Feb-11, Jun-11, and Dec-11 earthquake events, respectively, were used for all sites in this study.

Table 9a: Coverage area and height of ejecta estimates for Patch A (10-m buffer) using photographs.

Earthquake Event	$A_{E,thick}$ (m^2)	$H_{E,thick}$ (mm)	$A_{E,thin}$ (m^2)	$H_{E,thin}$ (mm)	A_T (m^2)
Sep-10	0	0	0	0	231
Feb-11	0	0	0	0	231
Jun-11	0	0	0	0	231
Dec-11	0	0	0	0	231

Notes: $A_{E,thick/thin}$ = Coverage area of thick/thin ejecta layers; $H_{E,thick/thin}$ = Lower-upper estimate of height of thick/thin ejecta layers; A_T = Total assessment area of a buffer being considered; Thin and thick layers correspond to light gray and dark gray colors of ejecta observed in aerial photographs.

Table 9b: Coverage area and height of ejecta estimates for Patch A (20-m buffer) using photographs.

Earthquake Event	$A_{E,thick}$ (m^2)	$H_{E,thick}$ (mm)	$A_{E,thin}$ (m^2)	$H_{E,thin}$ (mm)	A_T (m^2)
Sep-10	0	0	0	0	479
Feb-11	16	60-120	0	0	479
Jun-11	5.9	40-100	0	0	479
Dec-11	0	0	0	0	479

Notes: $A_{E,thick/thin}$ = Coverage area of thick/thin ejecta layers; $H_{E,thick/thin}$ = Lower-upper estimate of height of thick/thin ejecta layers; A_T = Total assessment area of a buffer being considered; Thin and thick layers correspond to light gray and dark gray colors of ejecta observed in aerial photographs.

Table 9c: Coverage area and height of ejecta estimates for Patch A (50-m buffer) using photographs.

Earthquake Event	$A_{E,thick}$ (m^2)	$H_{E,thick}$ (mm)	$A_{E,thin}$ (m^2)	$H_{E,thin}$ (mm)	A_T (m^2)
Sep-10	0	0	0	0	585
Feb-11	19	60-120	0	0	585
Jun-11	5.9	40-100	0	0	585
Dec-11	0	0	0	0	585

Notes: $A_{E,thick/thin}$ = Coverage area of thick/thin ejecta layers; $H_{E,thick/thin}$ = Lower-upper estimate of height of thick/thin ejecta layers; A_T = Total assessment area of a buffer being considered; Thin and thick layers correspond to light gray and dark gray colors of ejecta observed in aerial photographs.

Table 9d: Coverage area and height of ejecta estimates for Patch B (20-m buffer) using photographs.

Earthquake Event	$A_{E,thick}$ (m^2)	$H_{E,thick}$ (mm)	$A_{E,thin}$ (m^2)	$H_{E,thin}$ (mm)	A_T (m^2)
Sep-10	0	0	0	0	161
Feb-11	32	60-120	53	10-30	161
Jun-11	0	0	0	0	161
Dec-11	0	0	0	0	161

Notes: $A_{E,thick/thin}$ = Coverage area of thick/thin ejecta layers; $H_{E,thick/thin}$ = Lower-upper estimate of height of thick/thin ejecta layers; A_T = Total assessment area of a buffer being considered; Thin and thick layers correspond to light gray and dark gray colors of ejecta observed in aerial photographs.

Table 9e: Coverage area and height of ejecta estimates for Patch B (50-m buffer) using photographs.

Earthquake Event	$A_{E,thick}$ (m^2)	$H_{E,thick}$ (mm)	$A_{E,thin}$ (m^2)	$H_{E,thin}$ (mm)	A_T (m^2)
Sep-10	0	0	0	0	2208
Feb-11	294	60-120	393	10-30	2208
Jun-11	26.6	40-100	0	0	2208
Dec-11	0	0	0	0	2208

Notes: $A_{E,thick/thin}$ = Coverage area of thick/thin ejecta layers; $H_{E,thick/thin}$ = Lower-upper estimate of height of thick/thin ejecta layers; A_T = Total assessment area of a buffer being considered; Thin and thick layers correspond to light gray and dark gray colors of ejecta observed in aerial photographs.

Note 3: The values in Table 9 correspond to the coverage area of ejecta outlined in the aerial and satellite photographs (Figures 11, 12, 23, 25, 37, and 38) and the lower and upper estimates of ejecta height for similar nearby sites. The ejecta-induced settlement using photographs and engineering judgment, $S_{E,P}$, is estimated as

$$S_{E,P} = \frac{\sum_{i=1}^{a} A_{E,thick,i} * H_{E,thick,i} + \sum_{j=1}^{b} A_{E,thin,j} * H_{E,thin,j}}{A_T} = \frac{\sum_{i=1}^{a} V_{E,thick,i} + \sum_{j=1}^{b} V_{E,thin,j}}{A_T}$$

where

- $A_{E,thick,i}$ and $H_{E,thick,i}$ are the area and the height of a thick ejecta layer, respectively;
- $A_{E,thin,j}$ and $H_{E,thin,j}$ are the area and the height of a thin ejecta layer, respectively;
- A_T is the total assessment area for a buffer being considered (Figure 1).

Table 10a: Ejecta-induced settlement estimates for Patch A based on photographs.

Earthquake Event	Patch A (10-m buffer)		Patch A (20-m buffer)		Patch A (50-m buffer)	
	$S_{E,P,lower}$ (mm)	$S_{E,P,upper}$ (mm)	$S_{E,P,lower}$ (mm)	$S_{E,P,upper}$ (mm)	$S_{E,P,lower}$ (mm)	$S_{E,P,upper}$ (mm)
Sep-10	0	0	0	0	0	0
Feb-11	0	0	2	4	≈0	1
Jun-11	0	0	≈0	1	≈0	1
Dec-11	0	0	0	0	0	0

Note: $S_{E,P,lower}$ and $S_{E,P,upper}$ correspond to lower and upper estimates of $S_{E,P}$, respectively.

Table 10b: Ejecta-induced settlement estimates for Patch B based on photographs.

Earthquake Event	Patch B (20-m buffer)		Patch B (50-m buffer)	
	$S_{E,P,lower}$ (mm)	$S_{E,P,upper}$ (mm)	$S_{E,P,lower}$ (mm)	$S_{E,P,upper}$ (mm)
Sep-10	0	0	0	0
Feb-11	15	34	10	21
Jun-11	0	0	≈0	1
Dec-11	0	0	0	0

Note: $S_{E,P,lower}$ and $S_{E,P,upper}$ correspond to lower and upper estimates of $S_{E,P}$, respectively.

Table 11a: Best final estimates of ejecta-induced settlement for Patch A.

EQ Event	Patch A (10-m buffer)			Patch A (20-m buffer)			Patch A (50-m buffer)		
	$S_{E,L}$ (mm)	$S_{E,P}$ (mm)	$S_{E,final}$ (mm)	$S_{E,L}$ (mm)	$S_{E,P}$ (mm)	$S_{E,final}$ (mm)	$S_{E,L}$ (mm)	$S_{E,P}$ (mm)	$S_{E,final}$ (mm)
Sep-10	NA	0	0	NA	0	0	NA	0	0
Feb-11	NA	0	0	NA	3±1	5±5	NA	0.5±0.5	<5
Jun-11	ND	0	0	ND	0.5±0.5	<5	ND	0.5±0.5	<5
Dec-11	ND	0	0	ND	0	0	ND	0	0

Notes: $S_{E,L}$ = Ejecta-induced settlement based on LiDAR data reported in Table 8; $S_{E,P}$ = Median ejecta-induced settlement for the range of values reported in Table 10; $S_{E,final}$ = Best final estimate of ejecta-induced settlement rounded to the nearest 5; Final plus/minus values are also rounded to the nearest 5.

Table 11b: Best final estimates of ejecta-induced settlement for Patch B.

Earthquake Event	Patch B (20-m buffer)			Patch B (50-m buffer)		
	$S_{E,L}$ (mm)	$S_{E,P}$ (mm)	$S_{E,final}$ (mm)	$S_{E,L}$ (mm)	$S_{E,P}$ (mm)	$S_{E,final}$ (mm)
Sep-10	NA	0	0	NA	0	0
Feb-11	NA	25±10	25±10	NA	16±5	15±5
Jun-11	ND	0	0	ND	0.5±0.5	<5
Dec-11	ND	0	0	ND	0	0

Notes: $S_{E,L}$ = Ejecta-induced settlement based on LiDAR data reported in Table 8; $S_{E,P}$ = Median ejecta-induced settlement for the range of values reported in Table 10; $S_{E,final}$ = Best final estimate of ejecta-induced settlement rounded to the nearest 5; Final plus/minus values are also rounded to the nearest 5.

Table 11c: Best final estimates of ejecta-induced settlement for Patches A and B together.

Earthquake Event	Patch A+B (20-m buffer)			Patch A+B (50-m buffer)		
	$S_{E,L}$ (mm)	S_{E,P_avg} (mm)	$S_{E,final}$ (mm)	$S_{E,L}$ (mm)	S_{E,P_avg} (mm)	$S_{E,final}$ (mm)
Sep-10	NA	0	0	NA	0	0
Feb-11	NA	14±5	15±5	NA	8±3	10±5
Jun-11	ND	≈0	<5	ND	0.5±0.5	<5
Dec-11	ND	0	0	ND	0	0

Notes: $S_{E,L}$ = Ejecta-induced settlement based on LiDAR data reported in Table 8; $S_{E,P}$ = Median ejecta-induced settlement for the range of values reported in Table 10; $S_{E,final}$ = Best final estimate of ejecta-induced settlement rounded to the nearest 5; Final plus/minus values are also rounded to the nearest 5.

Note 4:

- $S_{E,final}$ for Patches A and B is based solely on $S_{E,P}$ for all earthquake events. There is no evidence of ejecta for the Sep-10, Jun-11, and Dec-11 earthquakes. For the Feb-11 earthquake, the Sep-10 LiDAR survey is not available, only aerial and satellite photographs.
- The LiDAR surveys did not capture the ground surface subsidence at the Barrington Park site for the Sep-10 and Feb-11 earthquakes, so they could not be used to estimate the ejecta-induced settlement for those two events. Moreover, the site is in the zone of severe to excessive LPI overprediction of liquefaction severity for both the Sep-10 and Feb-11 earthquake (Maurer et al. 2014[3]). The LDAT property inspection reports and ground photographs are not available for the site.

<u>Summary 1</u>:

The best estimate of the ejecta-induced free-field ground settlement at the Barrington Park site for the SEP 2010, FEB 2011, JUN 2011, and DEC 2011 earthquake is 0 mm, 15±5 mm, <5 mm, and 0 mm, respectively.

[3] Maurer, B. W., Green, R. A., Cubrinovski, M., & Bradley, B. A. (2014). Evaluation of the Liquefaction Potential Index for Assessing Liquefaction Hazard in Christchurch, New Zealand. *Journal of Geotechnical and Geoenvironmental Engineering*, 140(7), 04014032-1-11. doi:10.1061/(asce)gt.1943-5606.0001117

Figure 2: Location of the site.

Figure 3: Position of the site relative to nearby free-face features.

Figure 4: Position of the site relative to nearby buildings and vegetation.

Figure 5: Street view of the flat land.

Figure 6: Satellite image of the site taken in Apr 2004.

Figure 7: Satellite image of the site taken in Jan 2005.

Figure 8: Satellite image of the site taken in Jan 2006.

Figure 9: Satellite image of the site taken in Mar 2009.

Figure 10: Satellite image of the site taken in Oct 2009.

Figure 11: Satellite image of the site taken on Sep 3, 2010.

Figure 12: Satellite image of the site taken on Sep 5, 2010.

Figure 13: Satellite image of the site taken on Feb 15, 2011.

Figure 14: Satellite image of the site taken on Feb 23, 2011.

Figure 15: Satellite image of the site taken on Feb 26, 2011.

Figure 16: Satellite image of the site taken on Mar 28, 2011.

Figure 17: Satellite image of the site taken in Apr 2012.

Figure 18: Satellite image of the site taken in Mar 2013.

Figure 19: Satellite image of the site taken in Aug 2013.

Figure 20: Satellite image of the site taken in Nov 2015.

Figure 21: Aerial photograph of the site taken on Sep 4, 2010.

Figure 22: Aerial photograph of the site taken on Feb 24, 2011.

Figure 23: Aerial photograph of the site taken on June 14-15, 2011.

Figure 24: Aerial photograph of the site taken on June 16, 2011.

Figure 25: Aerial photograph of the site taken on Dec 24, 2011.

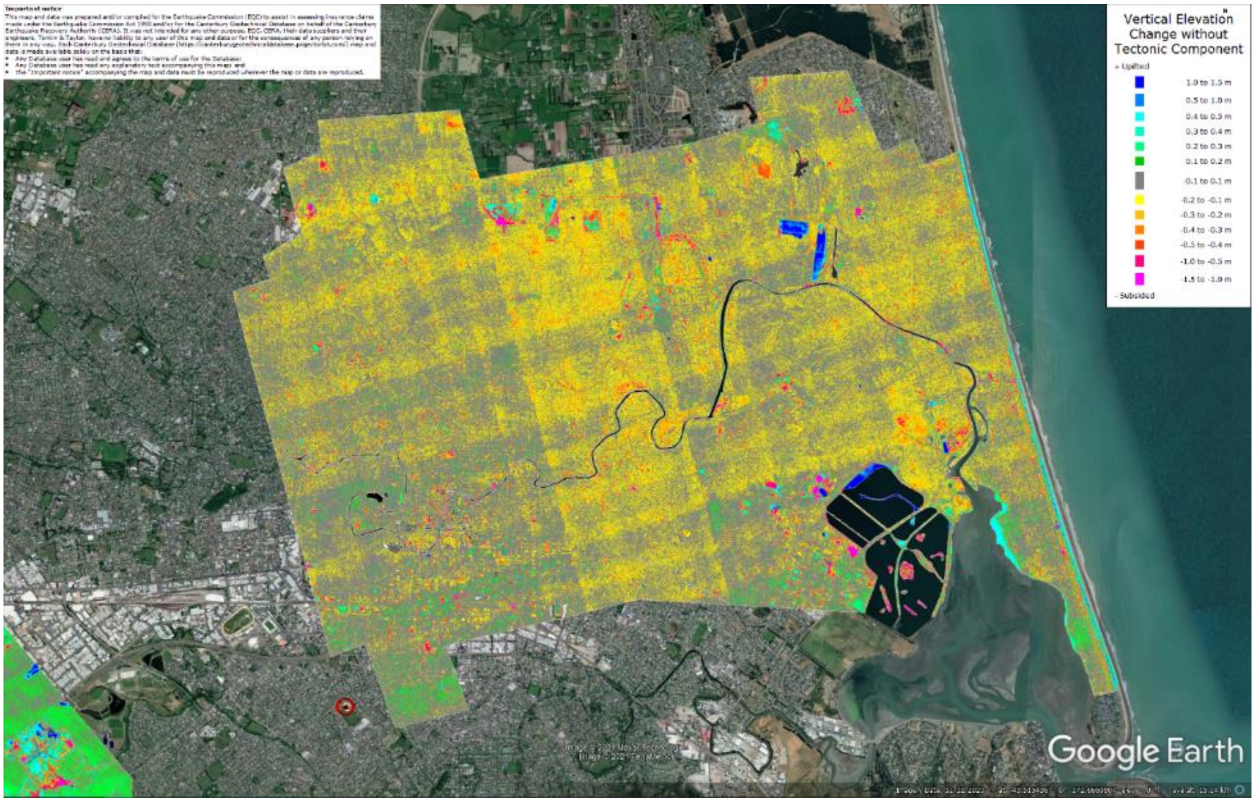

Figure 26: Vertical Ground Movements (Surface – Tectonic) for Sep 2010 Earthquake are not available.

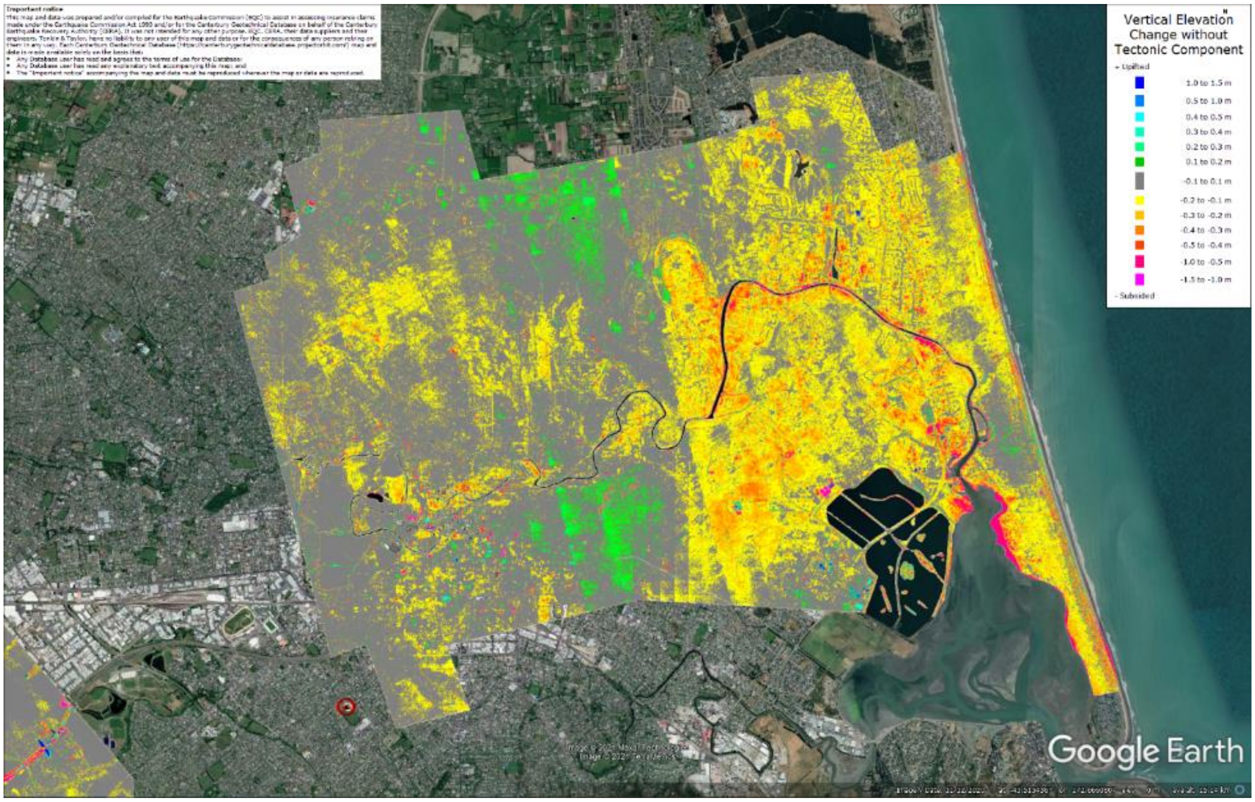

Figure 27: Vertical Ground Movements (Surface – Tectonic) for Feb 2011 Earthquake are not available.

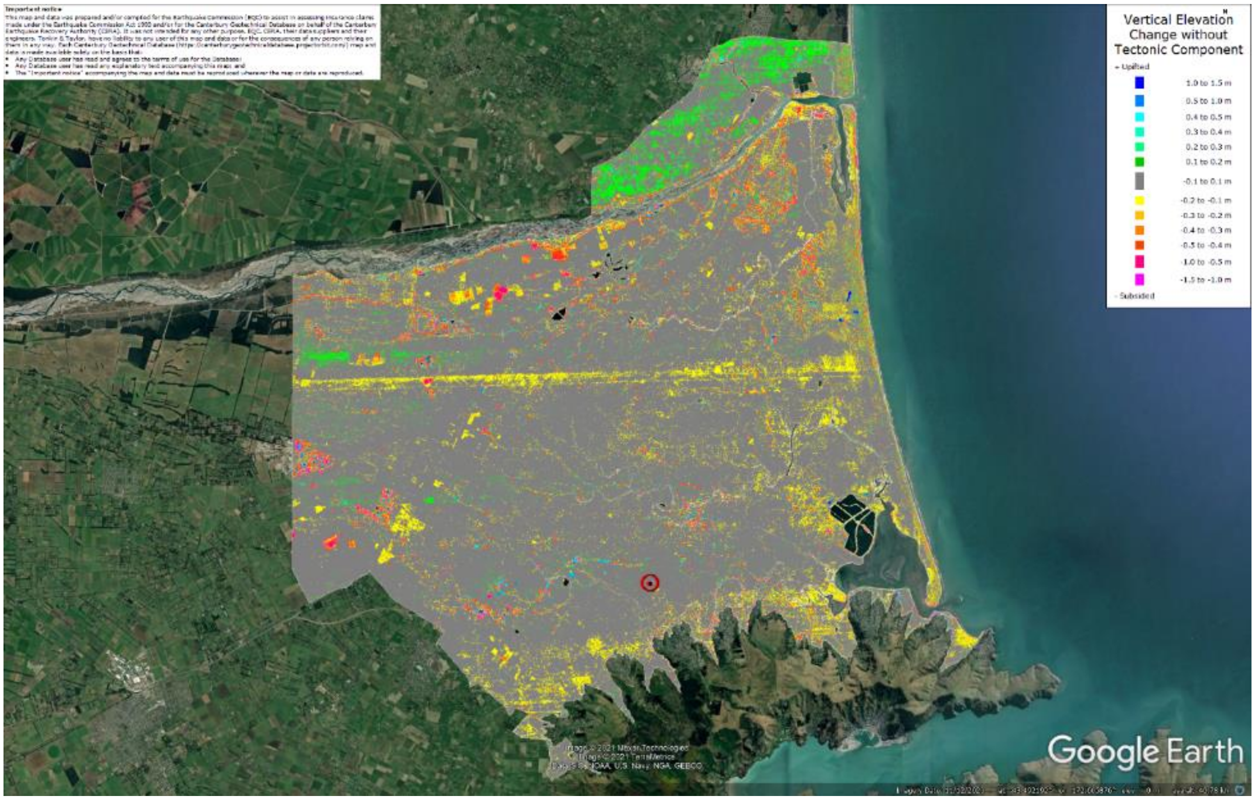

Figure 28: Vertical Ground Movements (Surface – Tectonic) for June 2011 Earthquake – the site is not in the apparent zone of overestimated or underestimated ground surface subsidence.

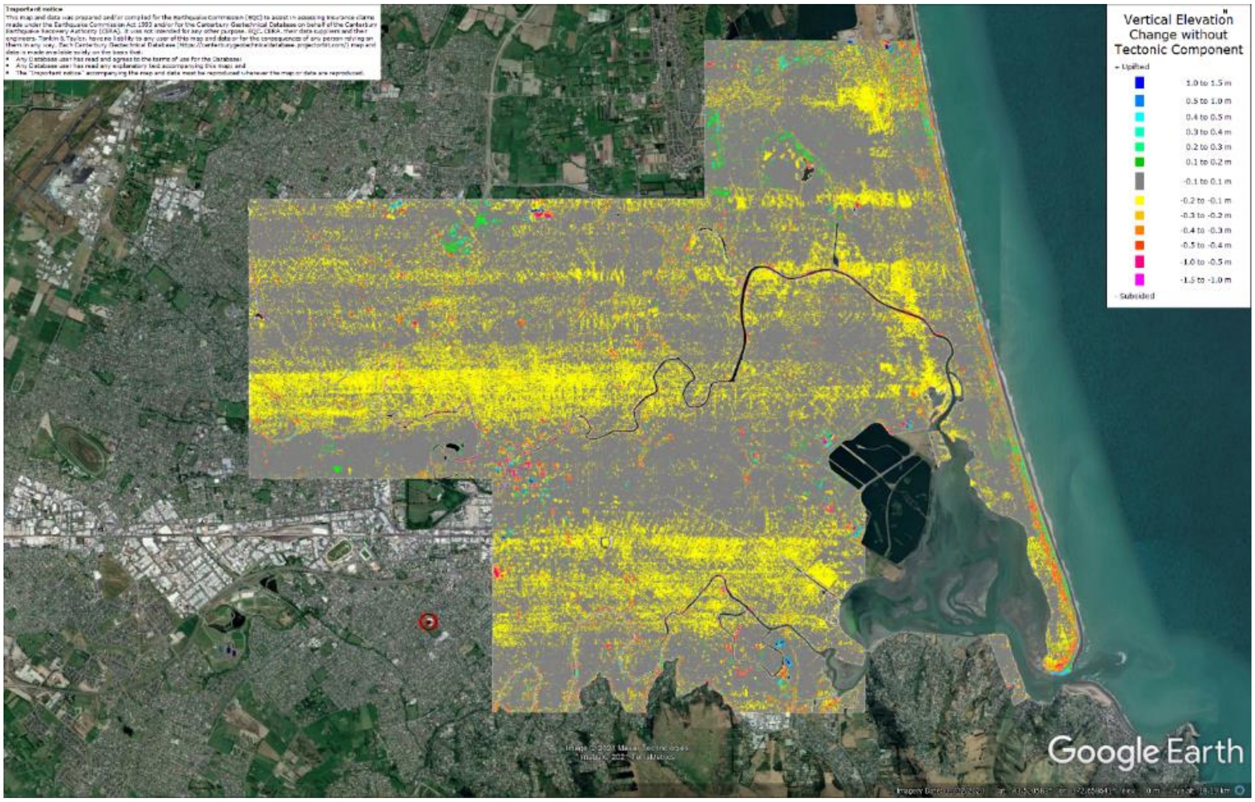

Figure 29: Vertical Ground Movements (Surface – Tectonic) for Dec 2011 Earthquake are not available.

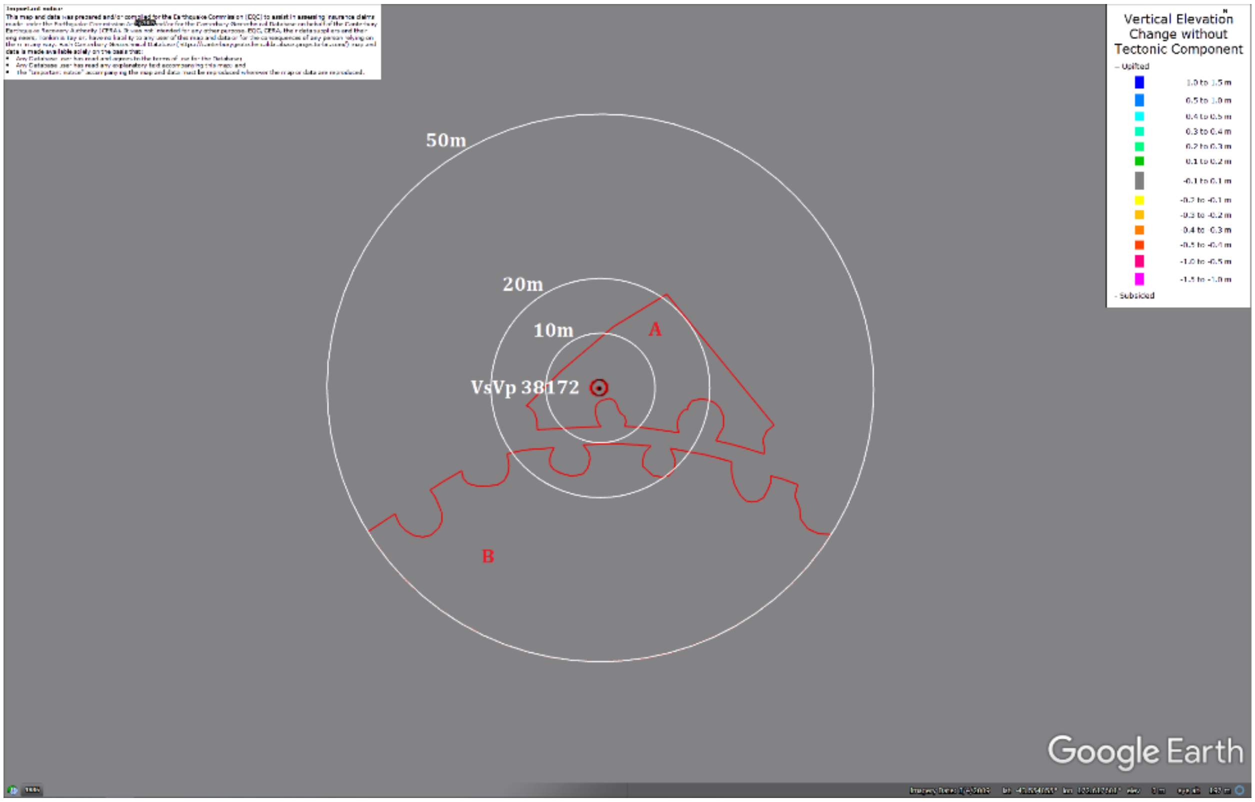

Figure 30: Ground surface subsidence without tectonic component for June 2011 Earthquake according to the LiDAR DEM.

Figure 31: No lateral spreading for Canterbury Earthquake Sequence.

Figure 32: Vertical tectonic movements for Sep 2010 Earthquake.

Figure 33: Vertical tectonic movements for Feb 2011 Earthquake.

Figure 34: Vertical tectonic movements for June 2011 Earthquake.

Figure 35: Vertical tectonic movements for Dec 2011 Earthquake.

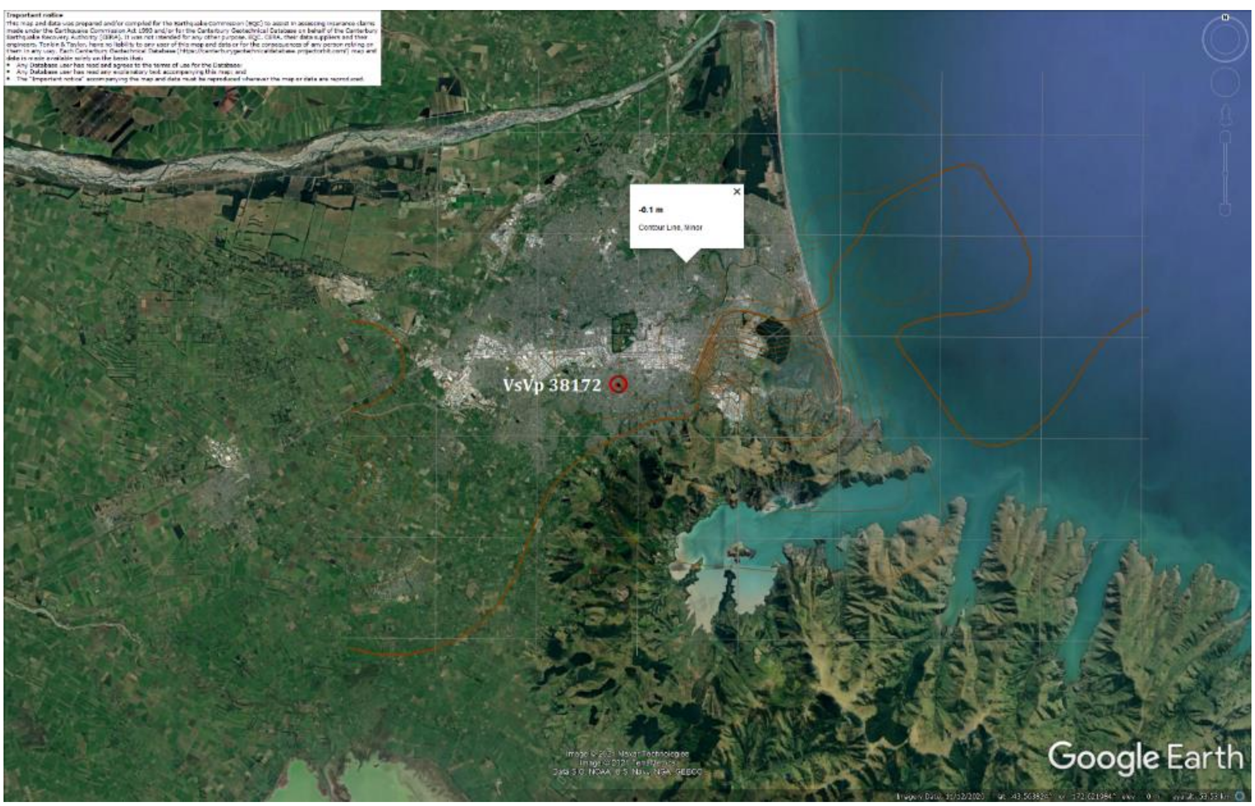

Figure 36: Vertical tectonic movements for Canterbury Earthquake Sequence.

Figure 37: Aerial photograph showing the ejecta outline at the site for Feb-11 EQ.

Figure 38: Aerial photograph showing the ejecta outline at the site for Jun-11 EQ.

Figure 39: PGA for Sep-10 EQ (st. dev. = 0.300-0.325 ln units).

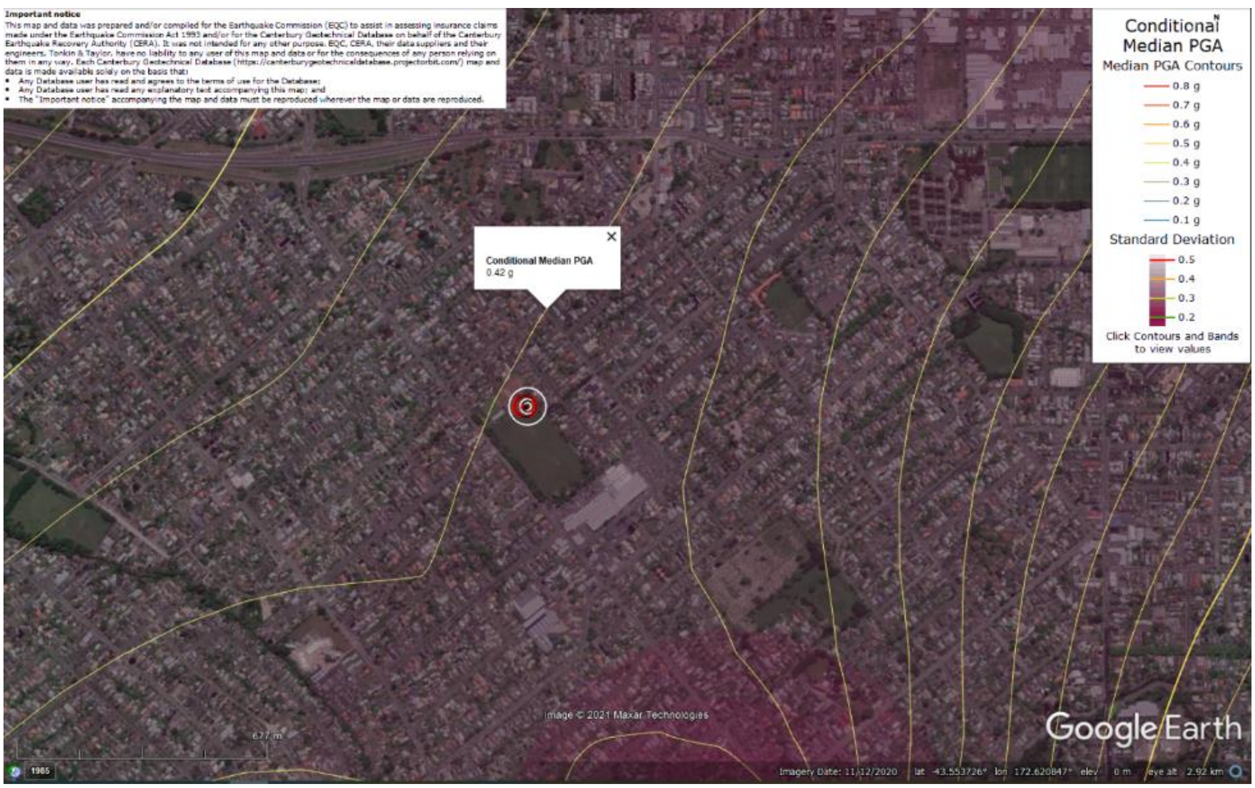

Figure 40: PGA for Feb-11 EQ (st. dev. = 0.325-0.350 ln units).

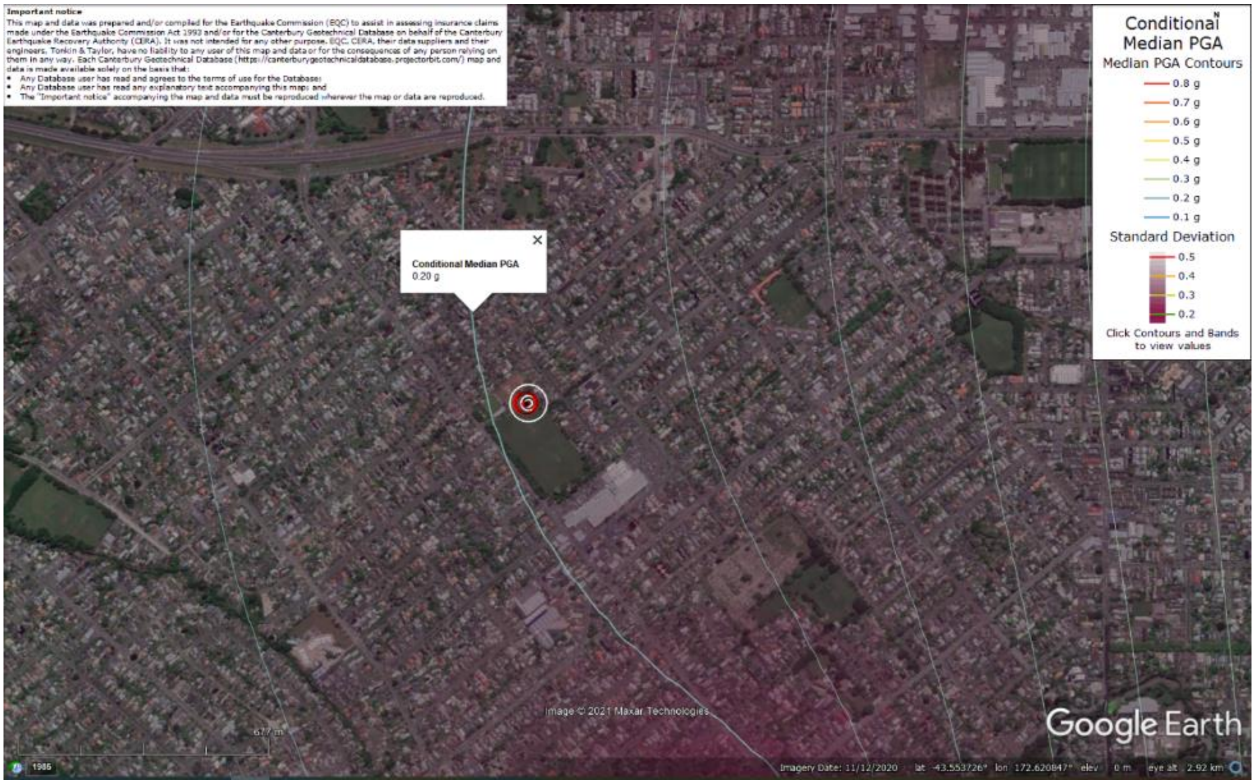

Figure 41: PGA for Jun-11 EQ (st. dev. = 0.350-0.375 ln units).

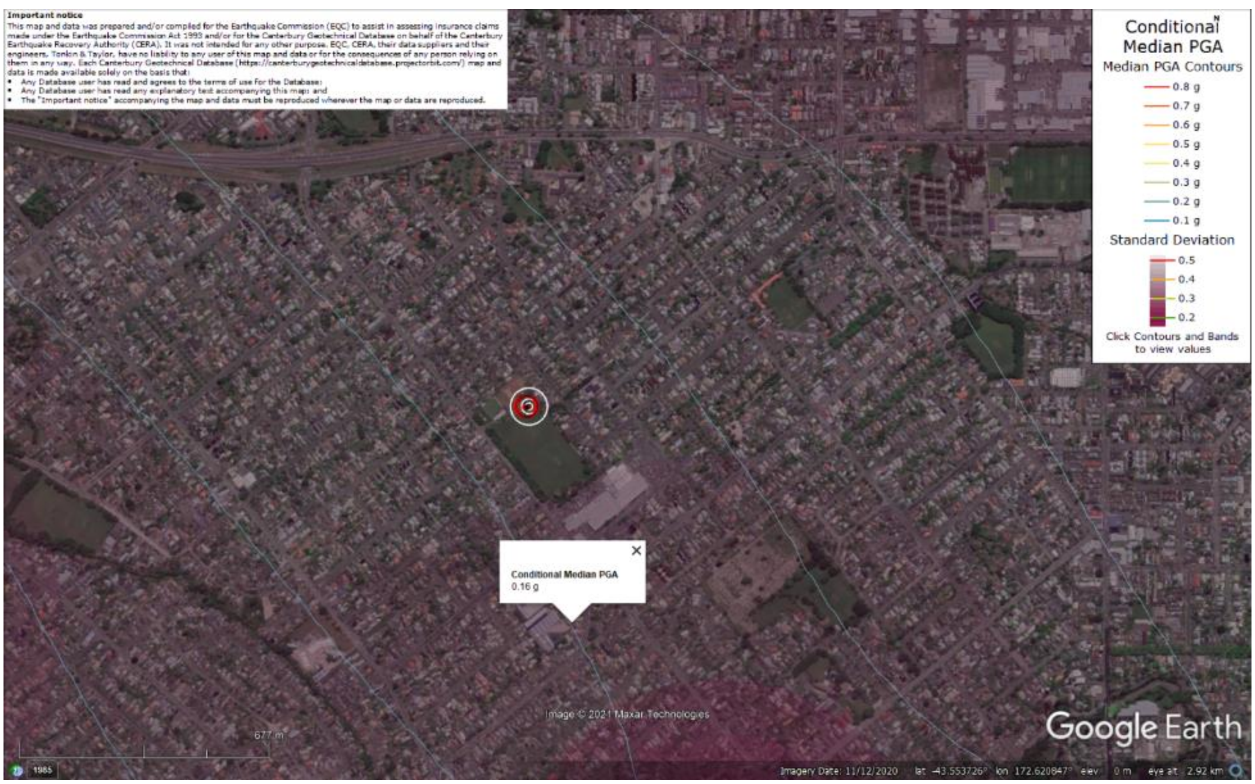

Figure 42: PGA for Dec-11 EQ (st. dev. = 0.350-0.375 ln units).

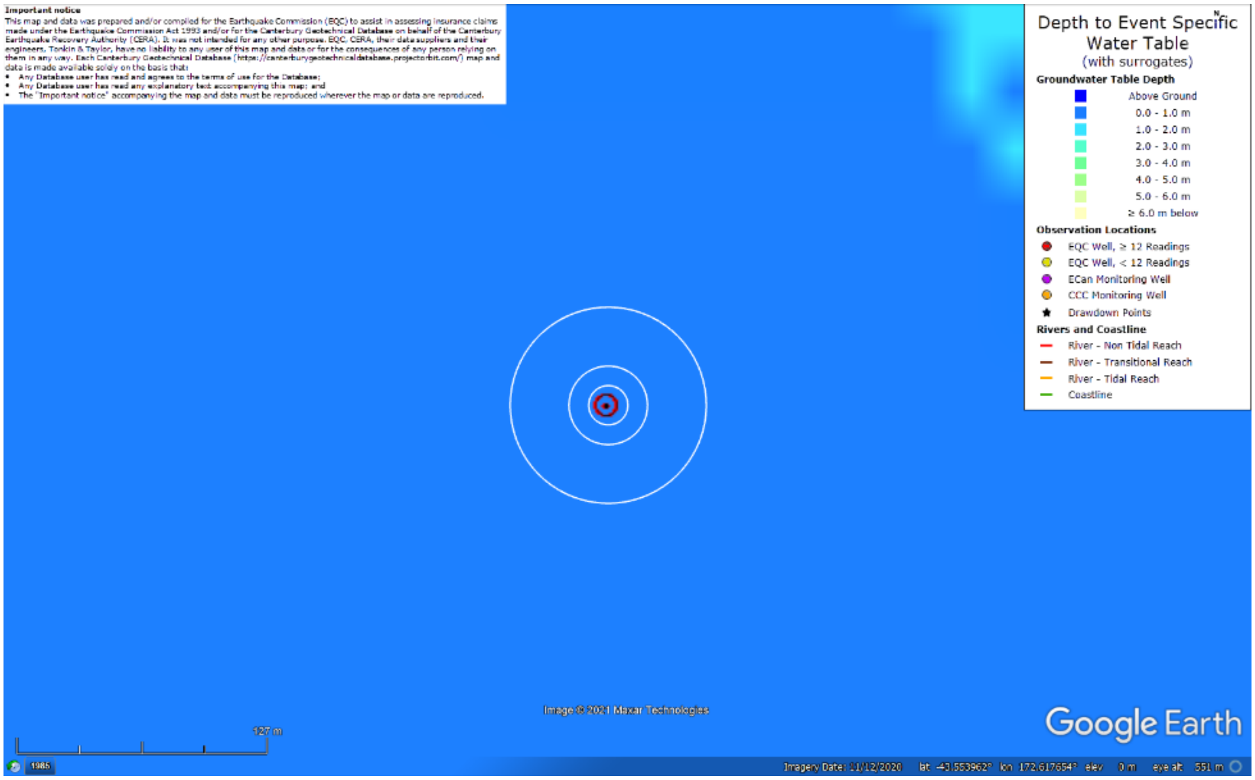

Figure 43: Depth to groundwater table for Sep-10 EQ.

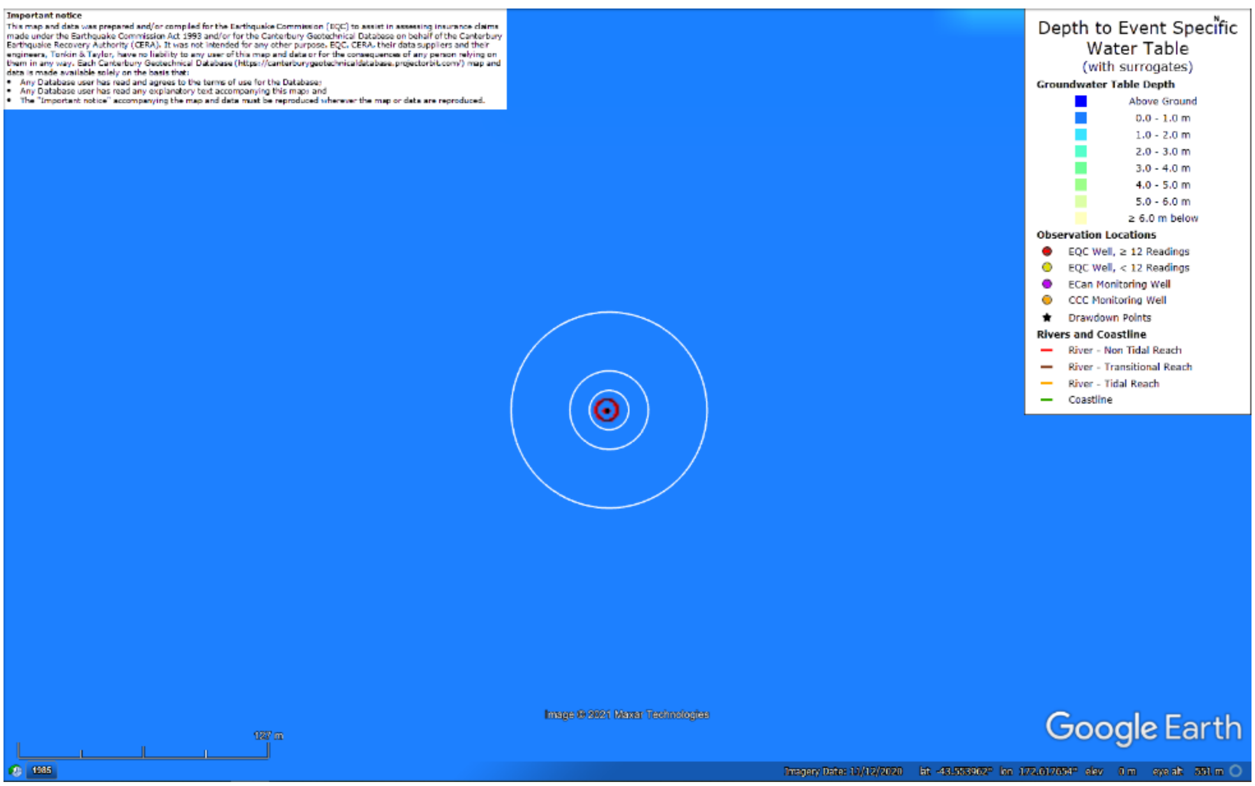

Figure 44: Depth to groundwater table for Feb-11 EQ.

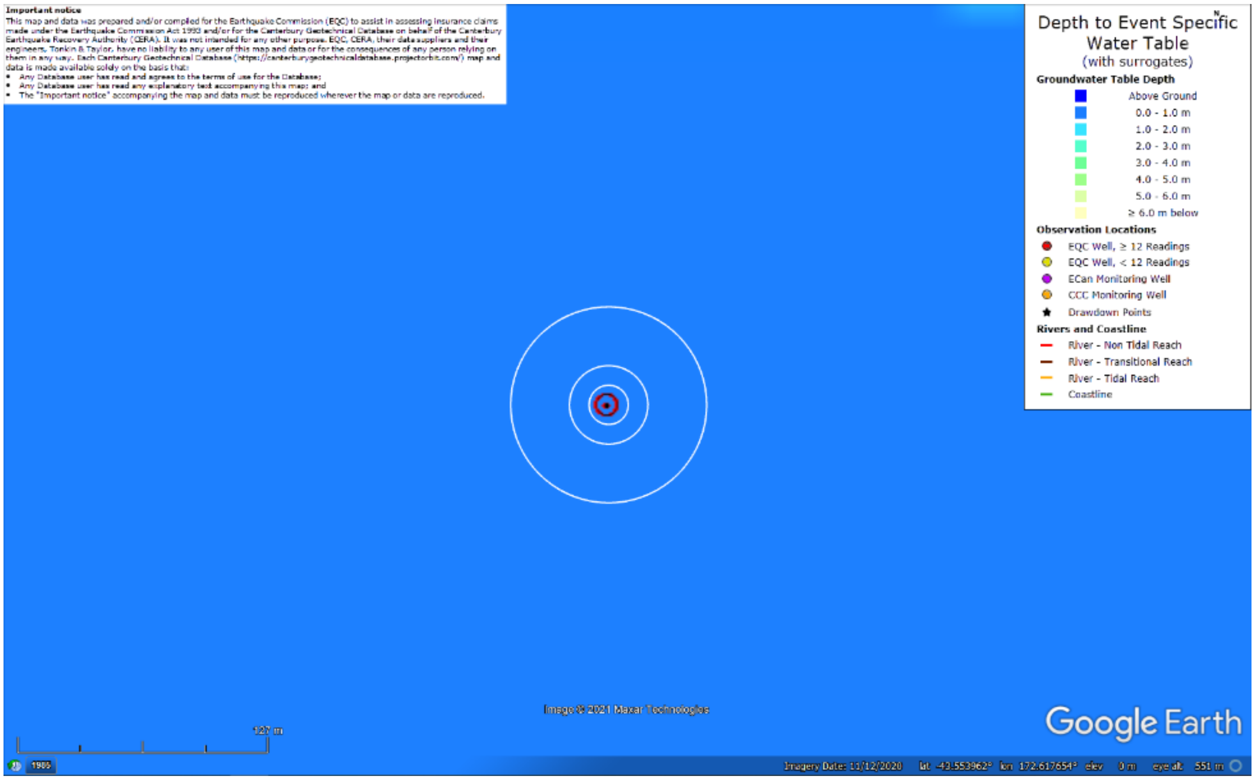

Figure 45: Depth to groundwater table for Jun-11 EQ.

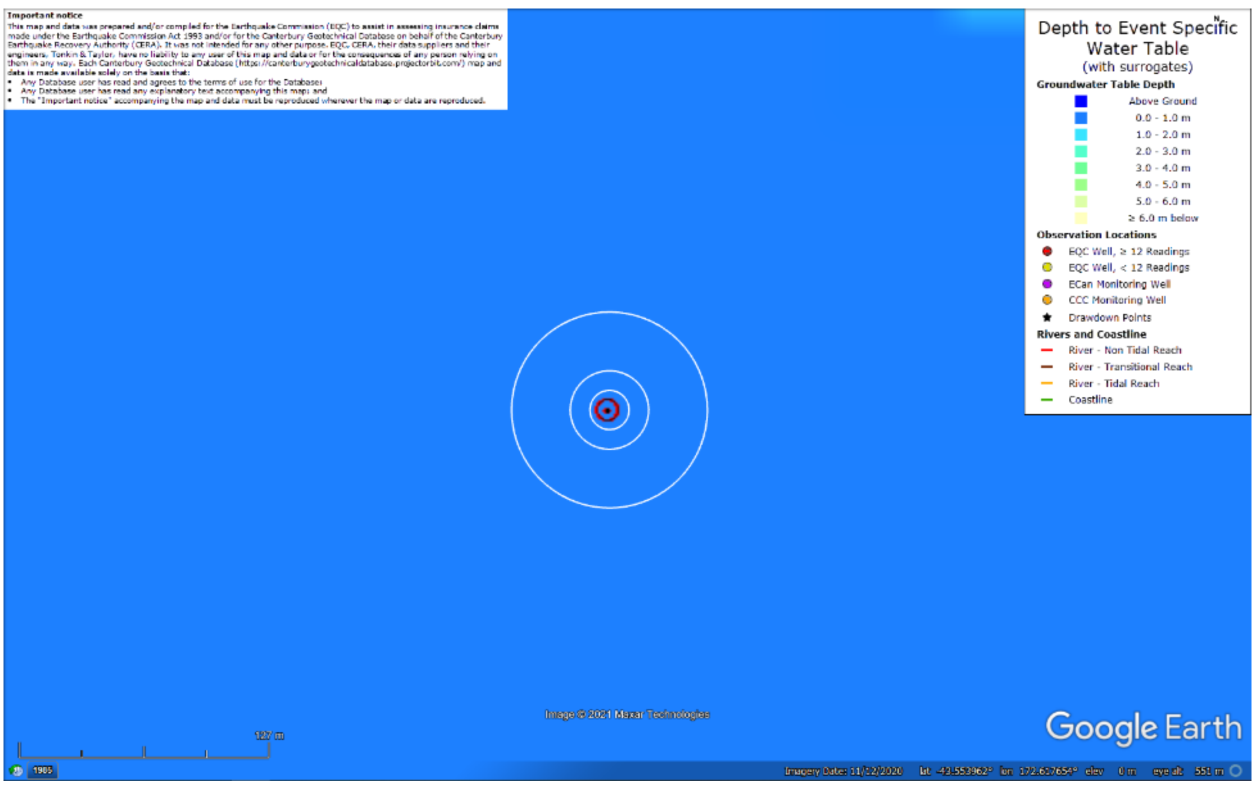

Figure 46: Depth to groundwater table for Dec-11 EQ.

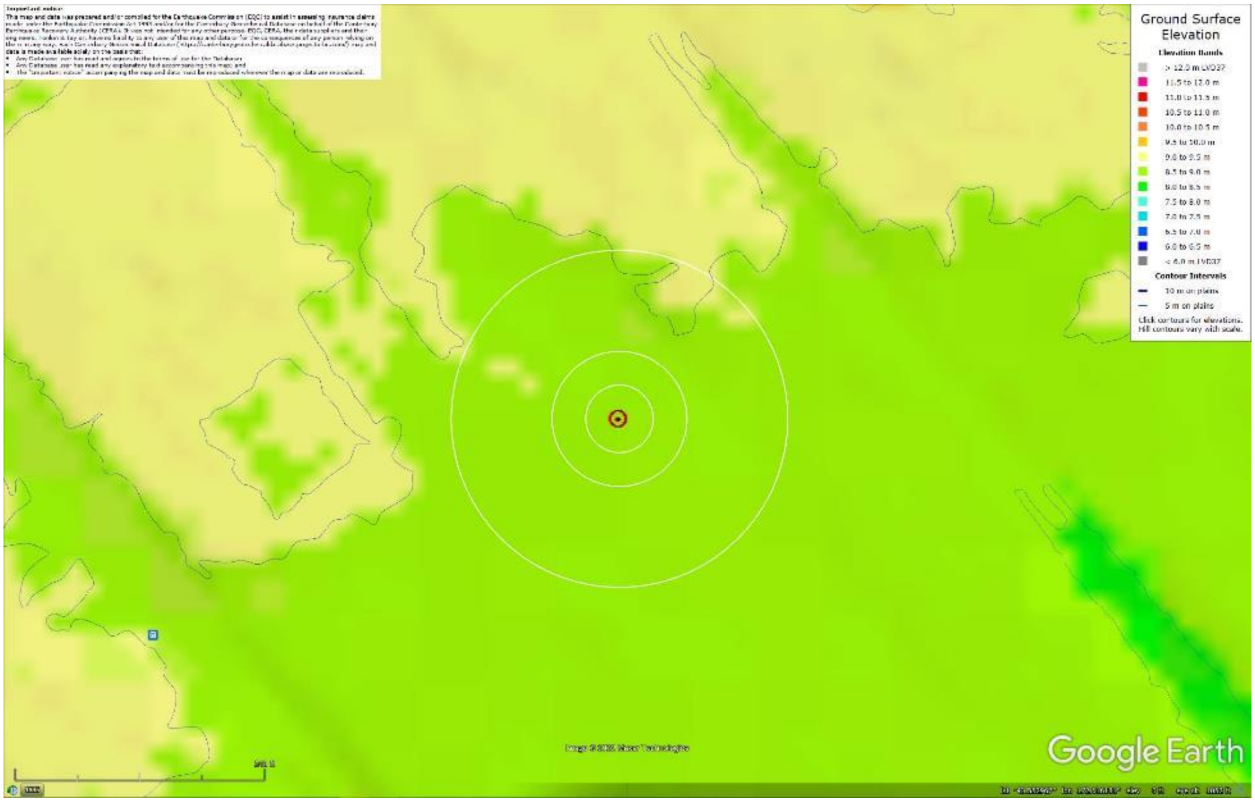

Figure 47: Ground surface elevation (Sep-11 LiDAR survey).

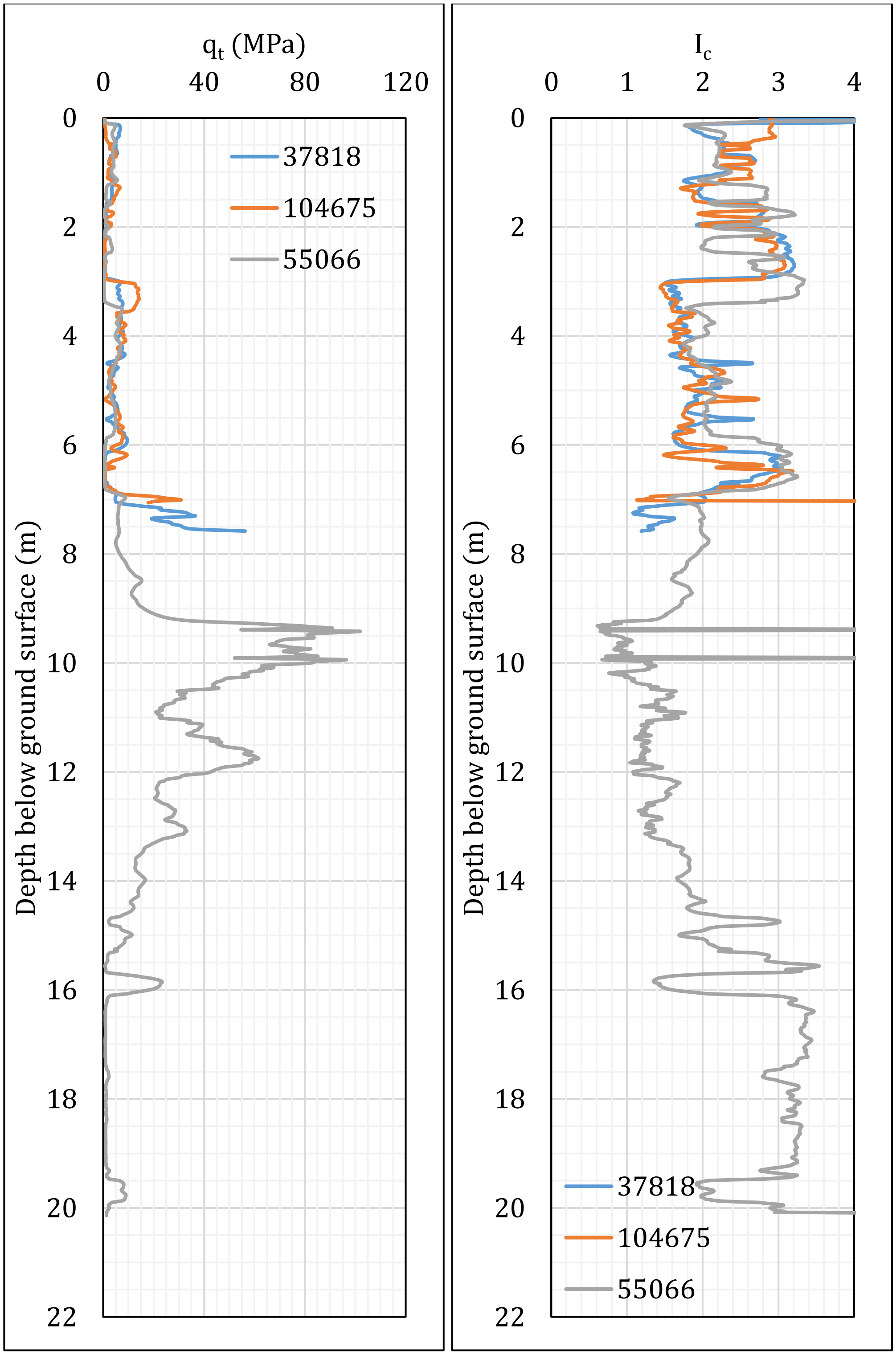

Figure 48: q_t and I_c profiles.

Note 5: The selection of CPTs for the area considered for settlement assessment (Figure 1) is based on the proximity of the CPTs to the considered areas. In accordance with that, the following table shows CPTs that were used for the volumetric settlement analysis in *Cliq v.3.0.3.2*, a CPT soil liquefaction software developed by GeoLogismiki. (The average volumetric settlements were reported in Table 8.)

Table 12: CPT profiles used in volumetric settlement analysis for areas selected for settlement assessment.

CPT ID No.	Patch A	Patch B
37818 (39724)	✓	✓
104675 (108756)	✓	✓
55066	✓	✓

Note: CPT 55066 (~330 m to the NE from the center of the site) was used to calculate the volumetric settlement below the layer of gravel for CPTs 37818 and 104675.

Table 13: CPT-based results.

EQ Event	Parameter	CPT ID 37818	CPT ID 104675	CPT ID 55066	Δ_{CPT}
Sep-10	S_{V1D} (mm)	84	68	99	18
	LSN	24	17	20	1
	LPI	9	7	8	0
	LPI_{ish}	7	5	4	--
	$D_{FS<1}$ (m)	1.24	3.57	2.17	--
Feb-11	S_{V1D} (mm)	98	83	132	28
	LSN	32	25	31	2
	LPI	18	15	18	1
	LPI_{ish}	15	8	12	--
	$D_{FS<1}$ (m)	0.88	1.38	0.79	--
Jun-11	S_{V1D} (mm)	54	44	51	5
	LSN	14	10	11	0
	LPI	3	2	2	0
	LPI_{ish}	2	0	1	--
	$D_{FS<1}$ (m)	2.94	4.26	2.17	--
Dec-11	S_{V1D} (mm)	22	18	19	1
	LSN	5	4	4	0
	LPI	0	0	0	0
	LPI_{ish}	0	0	0	--
	$D_{FS<1}$ (m)	4.78	undet.	4.77	--

Notes: $D_{FS<1}$ = Depth to the first liquefiable layer (FS_L<1) that is at least 200-mm thick, as determined by the Boulanger and Idriss (2016) liquefaction-triggering procedure (P_L=50%, C_{FC}=0.13, and $I_{c,cutoff}$ =2.6), and exported from *Cliq v.3.0.3.2*; undet. = the specified soil layer was not detected; Δ_{CPT} indicates the amount of S_{V1D}, LSN, and LPI to be added to CPTs 37818 and 104675, respectively, due to their shallow penetration depths.

Note 6: Based on the borehole log (BH 38193, Figure 1), the assumed groundwater table is at a depth of 1.45 m below the ground surface. The soil profile consists of (1) topsoil to a depth of 0.15 m, (2) silt, ML, the Yaldhurst member of the Springston formation, to a depth of 2.45 m , (3) silty fine sand, SM, the Yaldhurst member of the Springston formation, to a depth of 5.9 m, (4) silt, ML, the Yaldhurst member of the Springston formation, to a depth of 6.3 m, (5) silty fine sand, SM, the Yaldhurst member of the Springston formation, to a depth of 7.6 m, (6) fine to coarse gravel, GW, the Yaldhurst member of the Springston formation, to a depth of 9.85 m, and (7) fine to medium sand, SP, of the Christchurch formation to a depth of 10.0 m (the end of the borehole). According to the nearby borehole log (BH 18280 that is ~390 m to the NE from the center of the site), the fine to medium sand, SP, layer of the Christchurch formation continues to a depth of 12.9 m and is underlain by (8) fine to coarse gravel, GW, of the Christchurch formation to a depth of 15.15 m, (9) silty fine to medium sand, SM, of the Christchurch formation to a depth of 16.0 m, and (10) silt, ML, of the Christchurch formation to a depth of 20 m.

Note 7: The ejecta-induced free-field settlement provided in Table 11 is an areal average settlement due to ejecta, which is based on the total settlement assessment area, A_T (provided in Table 9 and repeated in Table 14). However, the considered area was not always covered completely with ejecta; thus, it is important to provide the localized ejecta-induced settlement, too. The localized settlement due to ejecta is estimated using photographic evidence only as

$$S_{E,P\_localized} = \frac{V_E}{A_E}$$

where V_E is the total volume of ejecta within A_T and A_E is the total coverage area of ejecta within A_T. Please note that the areal ejecta-induced settlement provided in Table 14 as S_{E,P_areal} is the same as $S_{E,P}$ in Table 11, which was estimated as

$$S_{E,P\_areal} = S_{E,P} = \frac{V_E}{A_T}$$

where V_E is the total volume of ejecta within A_T and A_T is the total settlement assessment area.

Table 14a: Areal and localized ejecta-induced settlement estimates for Patch A (20-m buffer) based on photographic evidence.

Earthquake Event	A_T (m^2)	A_E (m^2)	V_E (m^3)	S_{E,P_areal} (mm)	$S_{E,P\_localized}$ (mm)
Sep-10	479	0	0	0	0
Feb-11	479	16.0	1.0-1.9	5±5	90±30
Jun-11	479	5.9	0.2-0.6	<5	70±30
Dec-11	479	0	0	0	0

Notes: S_{E,P_areal} = $S_{E,P}$ reported in Table 11 = areal ejecta-induced settlement; $S_{E,P\_localized}$ = localized ejecta-induced settlement; A_T = total settlement assessment area; V_E = total volume of ejecta within A_T; A_E = total area of ejecta within A_T; The estimates of both areal and localized ejecta-induced settlement are rounded to the nearest 5; Final plus/minus values are also rounded to the nearest 5.

Table 14b: Areal and localized ejecta-induced settlement estimates for Patch A (50-m buffer) based on photographic evidence.

Earthquake Event	A_T (m^2)	A_E (m^2)	V_E (m^3)	S_{E,P_areal} (mm)	$S_{E,P\_localized}$ (mm)
Sep-10	585	0	0	0	0
Feb-11	585	19.0	0.2-0.6	<5	20±10
Jun-11	585	5.9	0.2-0.6	<5	70±30
Dec-11	585	0	0	0	0

Notes: S_{E,P_areal} = $S_{E,P}$ reported in Table 11 = areal ejecta-induced settlement; $S_{E,P\_localized}$ = localized ejecta-induced settlement; A_T = total settlement assessment area; V_E = total volume of ejecta within A_T; A_E = total area of ejecta within A_T; The estimates of both areal and localized ejecta-induced settlement are rounded to the nearest 5; Final plus/minus values are also rounded to the nearest 5.

Table 14c: Areal and localized ejecta-induced settlement estimates for Patch B (20-m buffer) based on photographic evidence.

Earthquake Event	A_T (m^2)	A_E (m^2)	V_E (m^3)	S_{E,P_areal} (mm)	$S_{E,P\_localized}$ (mm)
Sep-10	161	0	0	0	0
Feb-11	161	85.0	2.5-5.4	25±10	45±15
Jun-11	161	0	0	0	0
Dec-11	161	0	0	0	0

Notes: S_{E,P_areal} = $S_{E,P}$ reported in Table 11 = areal ejecta-induced settlement; $S_{E,P\_localized}$ = localized ejecta-induced settlement; A_T = total settlement assessment area; V_E = total volume of ejecta within A_T; A_E = total area of ejecta within A_T; The estimates of both areal and localized ejecta-induced settlement are rounded to the nearest 5; Final plus/minus values are also rounded to the nearest 5.

Table 14d: Areal and localized ejecta-induced settlement estimates for Patch B (50-m buffer) based on photographic evidence.

Earthquake Event	A_T (m^2)	A_E (m^2)	V_E (m^3)	S_{E,P_areal} (mm)	$S_{E,P\_localized}$ (mm)
Sep-10	2208	0	0	0	0
Feb-11	2208	687	21.6-47.1	15±5	50±20
Jun-11	2208	26.6	1.1-2.7	<5	70±30
Dec-11	2208	0	0	0	0

Notes: S_{E,P_areal} = $S_{E,P}$ reported in Table 11 = areal ejecta-induced settlement; $S_{E,P\_localized}$ = localized ejecta-induced settlement; A_T = total settlement assessment area; V_E = total volume of ejecta within A_T; A_E = total area of ejecta within A_T; The estimates of both areal and localized ejecta-induced settlement are rounded to the nearest 5; Final plus/minus values are also rounded to the nearest 5.

Summary 2:

The best estimate of the localized ejecta-induced free-field ground settlement at the Barrington Park site for the SEP 2010, FEB 2011, JUN 2011, and DEC 2011 earthquake is 0 mm, 70±15 mm, 35±15 mm, and 0 mm, respectively. The estimates for the FEB 2011 and JUN 2011 earthquake correspond to the average of the Patch A and Patch B 20-m buffer values.